

Design of allele-specific inhibitors to probe protein kinase signaling

Anthony C. Bishop*, Kavita Shah*, Yi Liu*, Laurie Witucki*, Chi-yun Kung* and Kevan M. Shokat*[†]

Background: Deconvoluting protein kinase signaling pathways using conventional genetic and biochemical approaches has been difficult because of the overwhelming number of closely related kinases. If cell-permeable inhibitors of individual kinases could be designed, the role of each kinase could be systematically assessed.

Results: We have devised an approach combining chemistry and genetics to develop the first highly specific cell-permeable inhibitor of the oncogenic tyrosine kinase v-Src. A functionally silent active-site mutation was made in v-Src to distinguish it from all other cellular kinases. A tight-binding cell-permeable inhibitor of this mutant kinase that does not inhibit wild-type kinases was designed and synthesized. *In vitro* and whole-cell assays established the unique specificity of the mutant v-Src–inhibitor pair. The inhibitor reversed cell transformation by the engineered but not the ‘wild type’ v-Src, establishing that changes in cellular signaling can be attributed to specific inhibition of the engineered kinase. The generality of the method was tested by engineering another tyrosine kinase, Fyn, to contain the corresponding active-site mutation to the one in v-Src. The same compound that inhibited mutant v-Src could also potentially inhibit the engineered Fyn kinase.

Conclusions: Allele-specific cell-permeable inhibitors of individual Src family kinases can be rapidly developed in an approach that should be applicable to all kinases. This approach will be useful for the deconvolution of kinase-mediated cellular pathways and for validating novel kinases as good targets for drug discovery both *in vitro* and *in vivo*.

Background

Protein phosphorylation is a central mediator of many different cell-signaling events. The dissection of kinase signaling pathways is a challenge to existing biochemical and genetic methods for several reasons. The pathways are highly interconnected, and biochemical studies of individual kinases have revealed remarkable functional similarities between kinases [1]. Also, many kinase gene knockouts have shown surprisingly mild phenotypes, either because kinases recognize substrates redundantly or because of compensation by other kinases during development [2–4]. Cell-permeable inhibitors that are highly specific for one protein kinase would provide several key advantages over the gene ‘knockout’ approach to enzyme inactivation. Inhibitor treatment allows the cell no time to compensate adaptively for the missing activity of the target kinase. In addition, small molecules can be administered to a cell in varying concentrations, allowing observation of the effects of partial as well as total inhibition of the target kinase. Finally, inhibition of kinase activity at the catalytic active site in the Src-homology 1 (SH1) domain would presumably not disrupt important cellular

localization and protein–protein binding interactions that are generally mediated through other domains [1].

Despite their value in signal-transduction research, highly selective kinase inhibitors have proven very difficult to obtain. This is presumably because of the enormous size of the kinase superfamily and the highly conserved nature of kinase active sites, which make the design of an inhibitor that targets a given kinase an enormously challenging combinatorial problem [1,5–7]. The development of kinase-specific inhibitors has been a major focus of anti-tumor drug discovery research because of the ubiquitous connection between oncogenic transformation and constitutively active protein kinases [8–10]. Recently, significant progress has been made in the synthesis and identification of molecules that can discriminate between different receptor tyrosine kinases. Molecules that are highly selective for epidermal growth factor receptor (EGF-R) [11,12], platelet-derived growth factor receptor (PDGF-R) [13] and fibroblast growth factor receptor (FGF-R) [14,15] tyrosine kinases have been identified. Importantly, crystal structures of inhibitors bound to

Addresses: *Department of Chemistry, Princeton University, Princeton, New Jersey 08544, USA.

[†]Department of Molecular Biology, Princeton University, Princeton, New Jersey 08544, USA.

Correspondence: Kevan M. Shokat
E-mail: shokat@princeton.edu

Received: 19 November 1997

Revised: 6 January 1998

Accepted: 19 January 1998

Published: 11 February 1998

Current Biology 1998, 8:257–266

<http://biomednet.com/eleceref/0960982200800257>

© Current Biology Ltd ISSN 0960-9822

kinases [15] and modeling studies [12,16] are facilitating the structure-based design of highly selective molecules. Despite these efforts, few inhibitors that are entirely specific for a single cytoplasmic protein kinase have been identified [17], and no general methods for specifically targeting a given kinase have been described.

We have devised a combined chemical and genetic strategy that allows for the generation of ‘chemical-sensitive’ mutant kinases each of which is uniquely inhibited by a rationally designed small-molecule inhibitor. Our approach involves engineering into the active site of the kinase of interest a unique ‘pocket’ resulting from the introduction of a functionally silent mutation. A specific inhibitor of the engineered kinase is then synthesized by derivatizing a known kinase inhibitor with a bulky chemical group designed to fit the novel active-site pocket. The bulky group prevents the compound from inhibiting wild-type kinases, which do not have the pocket. Successful complementary design therefore results in interactions between only the engineered kinase and the inhibitor. Transfection of cells with the gene encoding the engineered kinase generates cells in which only this one kinase can be blocked by the designed inhibitor (Figure 1). Importantly, because the mutant kinase has the same biological function as the wild-type kinase, an inhibitor of the mutant will affect cell signaling in the same manner as would a selective inhibitor of the endogenous kinase. The ability to observe the phenotype of cells after selective inhibition of a protein kinase provides a rapid method for determining the unique roles of individual kinases in signal-transduction cascades.

We have targeted the Src family of protein tyrosine kinases for specific inhibitor design because of their ubiquitous functional importance in cells [3,18]. Despite intense investigation, the roles of individual Src family members have been difficult to assess because many of them co-localize in cells and many have similar sequences. Although some potent inhibitors of Src family kinases are known [19,20], no molecules have been identified that can effectively discriminate (≥ 20 -fold selectivity for one Src family member) between these closely related enzymes [10].

Two Src kinases, v-Src and Fyn, were chosen as the primary targets of our mutant kinase–inhibitor pair design. Src kinase has emerged as a leading drug target because of its implication in the oncogenesis of breast, lung and colon cancers [10]. Although v-Src is the prototype for oncogenic tyrosine kinases, no small-molecule inhibitors that are highly selective for this kinase have been discovered [10]. Fyn is a Src family tyrosine kinase that is important in lymphocyte activation mediated by the T-cell receptor [3,21]. Src and Fyn share a similar domain structure and have approximately 85% amino-acid identity in their catalytic domains [22]. The close structural relationship of

the Src family members provides the ideal test of our ability to engineer enzyme–inhibitor specificity that can distinguish between highly homologous kinases. If one can discriminate between these closely related Src family members using a cell-permeable inhibitor, it is likely that specificity for members of other protein-kinase families can also be achieved using a similar approach.

Results and discussion

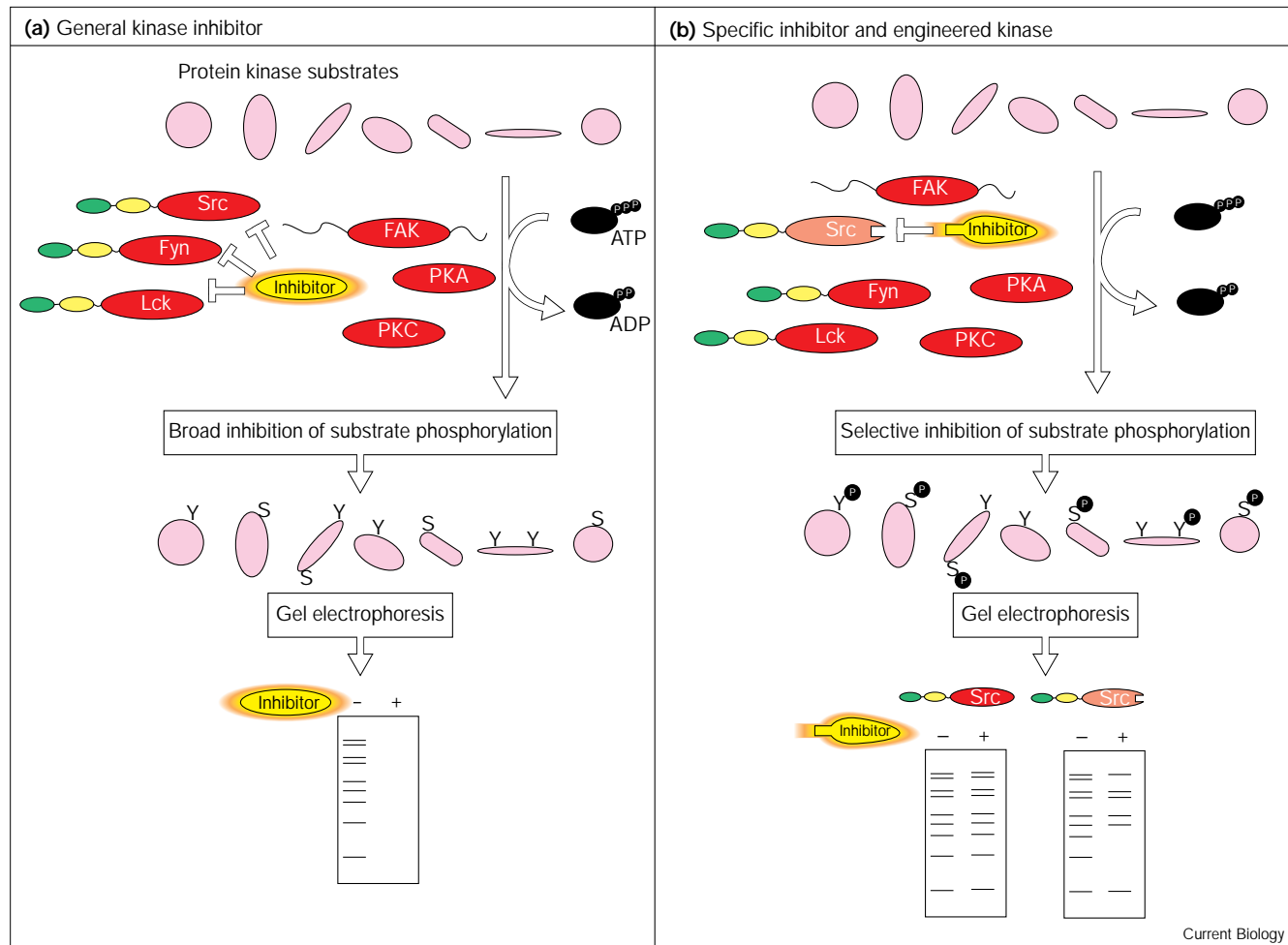
Enzyme engineering

From our previous efforts to engineer kinases with novel ATP specificity [23,24], we identified a functionally conserved residue (Ile 338) in the ATP-binding pocket of v-Src that could be mutated to glycine without altering the phosphoacceptor specificity or biological function of the kinase. The mutation (I338G) causes only a modest drop in the k_{cat} of v-Src, a modest increase in the K_m for ATP [24] and no quantitative change in the level of fibroblast transformation compared to the non-engineered (‘wild-type’) protein (K.S., unpublished observations). Crystal structures of ATP-bound protein kinases have in all cases revealed close contact and interaction between the residue corresponding to 338 in Src and ATP [25–28]. Analysis of protein kinase sequence alignments confirms that residue 338 contains a bulky side chain (usually threonine, isoleucine, leucine, methionine or phenylalanine) in all known eukaryotic protein kinases [29]. Thus, the mutation to glycine at residue 338 should create a novel pocket that is not present in any wild-type kinase. Because of the expanded ATP-binding site, the glycine mutant kinases should bind bulky inhibitors that could not bind wild-type kinases. Using standard methods, we cloned, expressed and purified the glutathione-S-transferase (GST) fusion protein of the wild-type and I338G v-Src catalytic domains as described [23,24]. Wild-type Fyn, T339G Fyn and the wild-type Abl tyrosine kinase were also expressed and purified as GST fusion proteins.

Inhibitor design and synthesis

To test our basic design strategy, we screened the wild-type and I338G v-Src SH1 domains against a previously synthesized panel of N-6-substituted adenosine molecules [23] for selective inhibition of I338G v-Src over wild-type v-Src. Because adenosine is only a moderate inhibitor of Src family tyrosine kinases, we did not expect to discover a potent inhibitor of the engineered kinase. As expected, all of the N-6 adenosine analogues inhibited I338G v-Src more potently than wild-type v-Src (data not shown). The most potent inhibitor found in this screen was N-6 cyclopentyladenosine (**1**, Figure 2a) with a 50% inhibitory concentration (IC_{50}) of 1 μ M for I338G v-Src. Subsequent experiments to test for selectivity demonstrated that N-6 cyclopentyladenosine showed no detectable *in vitro* inhibition of wild-type v-Src or Fyn at concentrations up to 400 μ M. This first screen encouraged us to pursue the strategy of developing novel inhibitors of

Figure 1



The specificity problems associated with using small-molecule protein-kinase inhibitors to deconvolute cell signaling. Kinase catalytic domains (red ovals) are highly conserved. Thus, **(a)** the majority of potent inhibitors block the activity of closely related kinases and broadly down-regulate pathways mediated by kinase activity. **(b)** The selective protein kinase inhibition approach described here. A space-creating mutation is introduced into the ATP-binding site of the kinase of choice

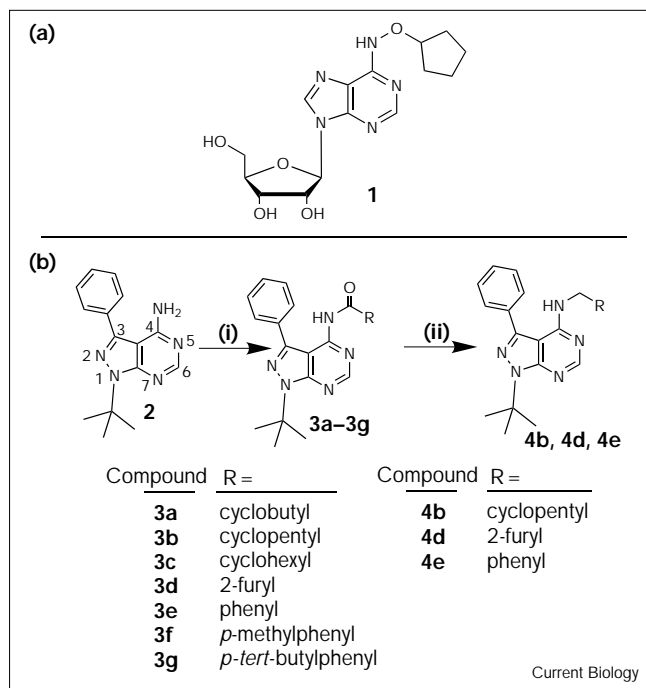
(Src). This mutation creates an active-site pocket in Src that can be uniquely recognized by the rationally designed small-molecule inhibitor. The inhibitor contains a bulky chemical group that makes it unable to bind wild-type protein kinases. Design of the complementary kinase–inhibitor pair allows for highly selective inhibition of the target kinase in the context of a whole cell. S indicates serine and Y indicates tyrosine.

I338G v-Src because our design had allowed us readily to overcome the selectivity barriers that are major problems in conventional inhibitor design.

As inhibitors, adenosine analogues are not ideal because adenosine performs many cellular functions and binds a large number of cellular proteins. N-6 adenosine analogues have been shown to act as adenosine-receptor agonists and antagonists [30], and N-6 adenosine analogues might conceivably act as substrates for nucleoside kinases. For these reasons, we turned to a class of known tyrosine-kinase inhibitors that are not direct analogues of biologically known molecules. Our design strategy called for a core

structure that exhibits potent inhibition of multiple wild-type kinases and is easily synthesized. Also, the binding orientation of the molecule in the enzyme active site must be known or readily predictable. In addition, the molecule must bind in a manner in which the site pointing toward Ile338 can be easily modified. As our core inhibitor structure we chose 4-amino-1-*tert*-butyl-3-phenylpyrazolo[3,4-*d*]pyrimidine (**2**, Figure 2b). This molecule is a derivative of 4-amino-1-*tert*-butyl-3-(*p*-methylphenyl)pyrazolo[3,4-*d*]pyrimidine (PP1) that was reported to be a potent Src family kinase inhibitor by Hanke and co-workers [19]. On the basis of the co-crystal structure of the Src family kinase Hck bound to the general kinase inhibitor quercetin

Figure 2



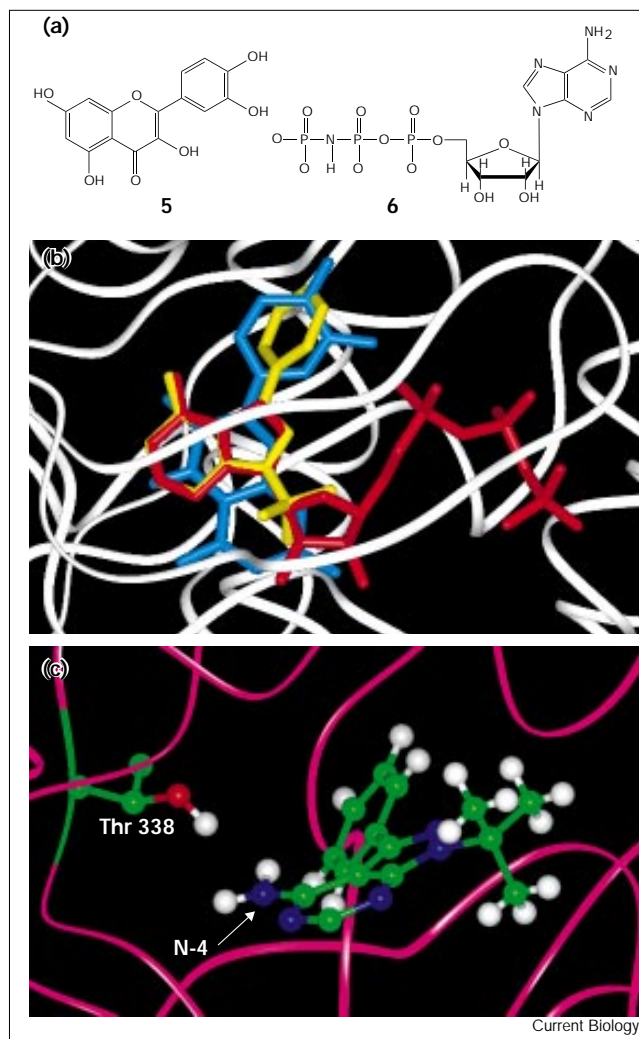
(a) Structure of N-6 cyclopentyladenosine (1). (b) Synthesis of pyrazolo[3,4-*d*]pyrimidine inhibitor analogues. Compound 2 was synthesized according to Hanefeld *et al.* [32]. (i) Acyl chloride (RCOCl; 10 equivalents), pyridine, 5°C, 1 h; then warm to 22°C, 11 h; (ii) LiAlH₄ (3.0 equivalents), dry tetrahydrofuran under argon, 0°C, 30 min; then heat to reflux for 30 min.

(5, Figure 3) [25,31], we postulated that 2 binds to Src family kinases in a conformation similar to that of ATP. The predicted binding orientation of 2 in Hck is shown in an overlay with the known Hck co-crystal structures of AMPPNP (6) and quercetin (Figure 3b) [25]. In this conformation, the easily derivatizable N-4 position of 2 corresponds to the N-6 of ATP (close contact with residue 338, Figure 3c) and the *tert*-butyl moiety roughly corresponds to the ribose ring of ATP. We further hypothesized that, in this orientation, the C-3 phenyl ring of 2 could bind in a pocket that surrounds the N-7 of ATP as seen in the Hck–quercetin co-crystal structure [25]. This analysis led us to synthesize a small panel of N-4 derivatized analogues of 2 [32,33] (Figure 2).

Identification of a uniquely selective inhibitor

The panel of pyrazolo[3,4-*d*]pyrimidines was screened against wild-type and I338G v-Src kinases (Table 1). All of the analogues were better inhibitors of the engineered v-Src than of wild-type v-Src, confirming our prediction of the binding orientation of 2 in the kinase active site. Any derivatization of 2 at the N-4 position destroyed the inhibitory activity against wild-type v-Src (no detectable inhibition at the limit of solubility, 300 μM). All 10 analogues demonstrated measurable inhibition of I338G

Figure 3



(a) Chemical structures of quercetin (5) and AMPPNP (6). (b) Predicted binding orientation of 2 in Src family kinase active sites. The crystal structures of Hck bound to AMPPNP (red) and Hck bound to quercetin (blue) were superimposed according to the Hck protein backbone (white) [25]. The structure of 2 (yellow) was subsequently docked into the kinase active site by superimposing the pyrazolo[3,4-*d*]pyrimidine ring system of 2 onto the adenine ring of AMPPNP. (c) Predicted close contact between N-4 of 2 and the side chain of residue 338 in Src family kinases. Molecule 2 has been docked into the ATP-binding site of the Src family kinase Hck as in (b). The atoms of the Thr338 side chain and 2 are colored according to their elemental make-up (green, carbon; blue, nitrogen; red, oxygen; white, hydrogen) and the Hck backbone is shown in pink. The methyl hydrogens of the threonine side chain are not shown. Images were generated using the program InsightII.

v-Src, and several of the compounds had IC₅₀ values in the low micromolar range. The N-4-(*p*-*tert*-butyl)benzoyl analogue (3g) was the most potent inhibitor of I338G v-Src in the panel (IC₅₀ = 430 nM). This molecule showed no inhibition of wild-type v-Src at 300 μM, suggesting that 3g is at least a 1000-fold better inhibitor of the mutant v-Src than

of wild-type v-Src. The size of the derivatization needed to achieve sub-micromolar potency for the I338G v-Src active site was rather unexpected. We removed only four carbon atoms from the ATP-binding site of the protein and added 11 carbon atoms to the parent molecule. This discrepancy may be due to an imperfection in our binding prediction. Alternatively, the isoleucine to glycine mutation may confer greater flexibility on the enzyme active site, allowing the mutant kinase to accept a larger inhibitor analogue than predicted [24]. To confirm that **3g** does inhibit I338G v-Src at the ATP-binding site, we investigated the kinetics of inhibition at various ATP concentrations. Lineweaver–Burk analysis confirmed that **3g** does inhibit I338G v-Src competitively with respect to ATP with an inhibitory constant (K_i) of 380 nM (data not shown).

The 10 inhibitor analogues were then screened against wild-type Fyn to investigate their potential to cross-react with this kinase. Wild-type Fyn was chosen as the ‘worst case’ control of wild-type kinases because both **2** and its parent molecule, PP1, are highly potent (low nanomolar) inhibitors of Fyn [19]. Many of the inhibitor analogues were not highly selective for the target kinase (Table 1). The N-acyl analogues with saturated ring systems (**3a–3c**) effectively inhibited wild-type Fyn. The N-methylene compounds (**4b–4e**) were sufficiently inactive against wild-type Fyn but showed only poor to moderate inhibition of I338G v-Src. Importantly, **3g**, the most potent inhibitor of the mutant v-Src, inhibited wild-type Fyn very weakly ($IC_{50} = 300 \mu\text{M}$). Thus, **3g** inhibits the engineered v-Src over 700 times more effectively than it inhibits wild-type Fyn, which is likely to be the wild-type cellular kinase that is the most capable of binding the molecule. We also tested whether other non-Src family kinases were fortuitously inhibited by **3g** *in vitro*. Inhibition of the serine/threonine kinases protein kinase C δ (PKC δ) and protein kinase A was not detected at inhibitor concentrations up to 300 μM . Likewise, **3g** exhibited only weak inhibition ($IC_{50} > 300 \mu\text{M}$) of Abl. The **3g** compound therefore satisfied all of our initial design requirements for potent selective inhibition of one engineered kinase.

Selectivity in whole cells

To demonstrate further that **3g** does not inhibit wild-type tyrosine kinases, we investigated the effects of **3g** treatment on the phosphorylation cascade triggered by activation of the B-cell receptor. Src family (Fyn, Lyn, Lck, Blk) and non-Src family (Btk, Syk) tyrosine kinases are known to be activated upon cross-linking of the B-cell receptor [34]. Because of the amplifying nature of the B-cell receptor signaling cascade, inhibition of any of the downstream kinases would dramatically alter the distribution and intensity of post-activation cellular phosphotyrosine [35]. Because **3g** was designed to be sterically incompatible with the active sites of wild-type kinases, it should not disrupt tyrosine-phosphorylation-dependent signaling in

wild-type B cells. Figure 4 shows that treatment of murine B cells that had had their antigen receptor cross-linked with 100 μM **3g** had no effect on the phosphotyrosine pattern of B-cell stimulation (compare lane 3 to lane 2). The signal intensities of all the major bands were unchanged and only slight depletion of some minor bands is detectable, confirming that **3g** does not appreciably inhibit the panel of tyrosine kinases that are activated by cross-linking the B-cell receptor. Treatment of B cells with 100 μM **2**, however, caused a significant reduction in tyrosine phosphorylation (Figure 4, lane 4) that is consistent with the ability of **2** to potently inhibit wild-type Src family kinases [19].

Selective inhibition of I338G v-Src in NIH3T3 cells

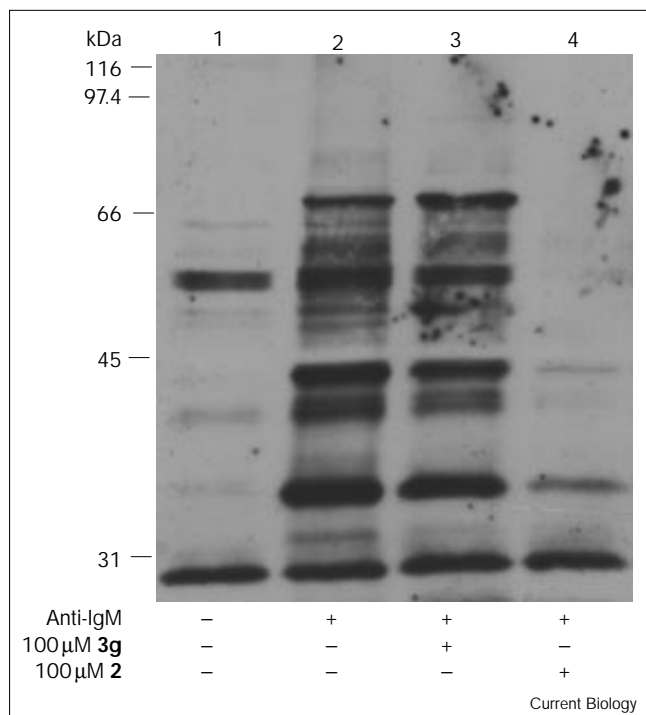
In order to use our selective inhibitor to study a Src-mediated pathway, we delivered genes encoding either wild-type or I338G v-Src into NIH3T3 fibroblasts via retrovirus infection [36]. These cells acquired a transformed phenotype that was dependent on v-Src expression. We sought to show that **3g** could selectively inhibit the Src-dependent signal-transduction pathway of I338G v-Src transformed cells but not affect cells transformed with wild-type v-Src. Cells infected with wild-type v-Src showed no loss of tyrosine phosphorylation when treated with 100 μM **3g** compared to control treatment with dimethyl sulfoxide (DMSO; Figure 5), demonstrating that **3g** does not inhibit wild-type v-Src or any of the other tyrosine kinases that are activated by v-Src-mediated

Table 1

***In vitro* IC₅₀ values of wild-type and engineered v-Src and Fyn peptide phosphorylation by pyrazolo[3,4-*d*]pyrimidine analogues.**

R =	Compound	IC ₅₀ (μM)			
		v-Src	I338G v-Src	Fyn	T339G Fyn
	3a	> 300	12	6.5	5
	3b	> 300	19	80	9
	4b	> 300	75	> 300	100
	3c	> 300	20	50	5
	3d	> 300	150	15	19
	4d	> 300	250	> 300	26
	3e	> 300	10	300	11
	4e	> 300	85	> 300	63
	3f	> 300	10	300	6
	3g	> 300	0.43	300	0.83

Figure 4



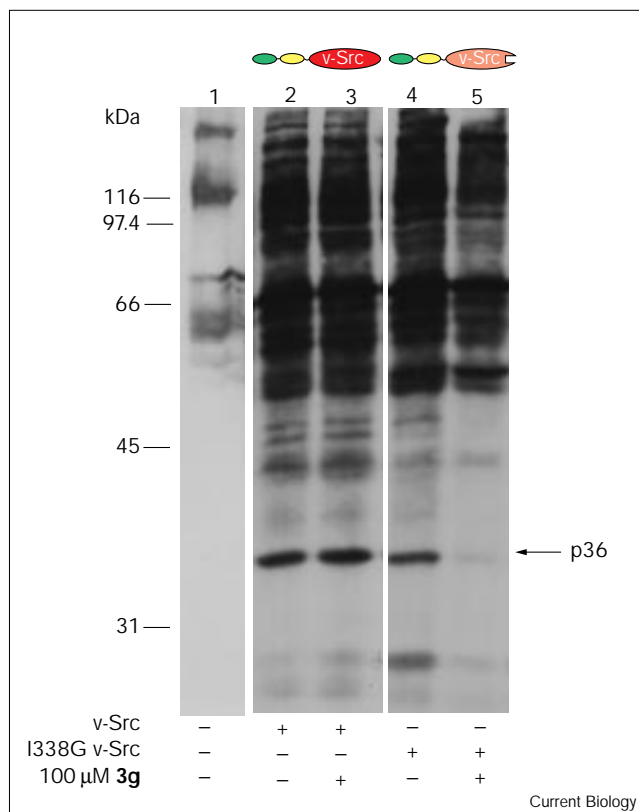
Inhibitor analogue **3g** does not inhibit tyrosine phosphorylation triggered by the active B-cell receptor. Murine spleen cells were incubated with 1.1% DMSO (lanes 1,2), 100 µM **3g** in 1.1% DMSO (lane 3), or 100 µM **2** in 1.1% DMSO (lane 4). B-cell stimulation (lanes 2–4) was initiated by the addition of 10 µg/ml goat anti-mouse IgM. Cellular proteins were resolved by 10% SDS-PAGE, transferred to nitrocellulose, and immunoblotted with a monoclonal anti-phosphotyrosine antibody (4G10).

cellular transformation. When cells infected with I338G v-Src were treated with 100 µM **3g**, there was a dramatic decrease in the tyrosine phosphorylation of the putative v-Src substrate, p36, as well as a moderate overall decrease in the cellular level of phosphotyrosine (Figure 5, lanes 4,5). It has been shown previously that treatment of v-Src-transformed cells with general tyrosine kinase inhibitors causes a reduction in the tyrosine phosphorylation of a 36 kDa protein [31]. It is thought that p36 is associated with a specific phosphotyrosine phosphatase, possibly explaining its rapid dephosphorylation in inhibitor-treated cells [37]. The IC_{50} of **3g** for the p36 phosphotyrosine signal in cells expressing I338G v-Src was ~50 µM, roughly 100 times the *in vitro* value (data not shown). This is presumably because the inhibitor must compete for the kinase active site with millimolar concentrations of ATP in the cellular environment [9].

Selective inhibition of I338G v-Src reverses transformed cell morphology

The activity of v-Src is required for the transformation of mammalian cells by the Rous sarcoma virus [38,39].

Figure 5



Inhibitor **3g** blocks p36 phosphorylation in NIH3T3 fibroblasts transformed with I338G v-Src but not wild-type v-Src. Non-transformed NIH3T3 cells (lane 1), wild-type v-Src-transformed NIH3T3 cells (lanes 2,3), and I338G v-Src-transformed NIH3T3 cells (lanes 4,5) were incubated with 1.1% DMSO (lanes 1,2,4) or 100 µM **3g** in 1.1% DMSO (lanes 3,5). After 12 h, the cells were lysed and protein phosphorylation levels determined as in Figure 4.

Treatment of NIH3T3 cells expressing I338G v-Src with 100 µM **3g** caused dramatic changes in cell morphology that are consistent with the reversal of transformation (Figure 6); the cells appeared flat and did not exhibit the growth characteristics of transformed cells (that is, the ability to grow on top of one another). Under identical conditions, cells infected with wild-type v-Src demonstrated the typical rounded morphology and overlapping growth patterns of transformed cells.

To demonstrate further the selective reversal of cell morphology, we used fluorescence microscopy to view **3g**-treated cells after staining the cellular polymerized actin with fluorescein isothiocyanate-phalloidin (Figure 6). Non-transformed NIH3T3 cells have long actin fibers that form across the cells [40]. Cells transformed with v-Src (both wild-type and I338G forms) appeared rounded with no discernible pattern of actin fibers. In agreement with the light microscopy data, inhibitor-treated cells expressing wild-type v-Src appeared indistinguishable from

untreated wild-type v-Src cells. The **3g**-treated cells expressing I338G v-Src had defined polymerized actin strings, however, which strongly resembled the actin formations of non-transformed NIH3T3 fibroblasts. These **3g**-treated cells had an exaggerated flattened morphology and showed peripheral actin staining that was not present in the non-transformed NIH3T3 cells. These data show that **3g** can induce morphological changes in cells that are engineered to contain a single amino-acid change in the kinase of interest. This is the first demonstration that a small-molecule inhibitor selective for a tyrosine-kinase oncogene product can revert the morphological changes associated with cellular transformation. Previous examples of morphological reversion of transformation by herbimycin A (and other benzoquinone ansamycins) have recently been shown to operate via a mechanism that is not related to kinase inhibition and consists of targeting of the oncogenic tyrosine kinase to the proteasome by use of the heat-shock protein Hsp90 [41–44].

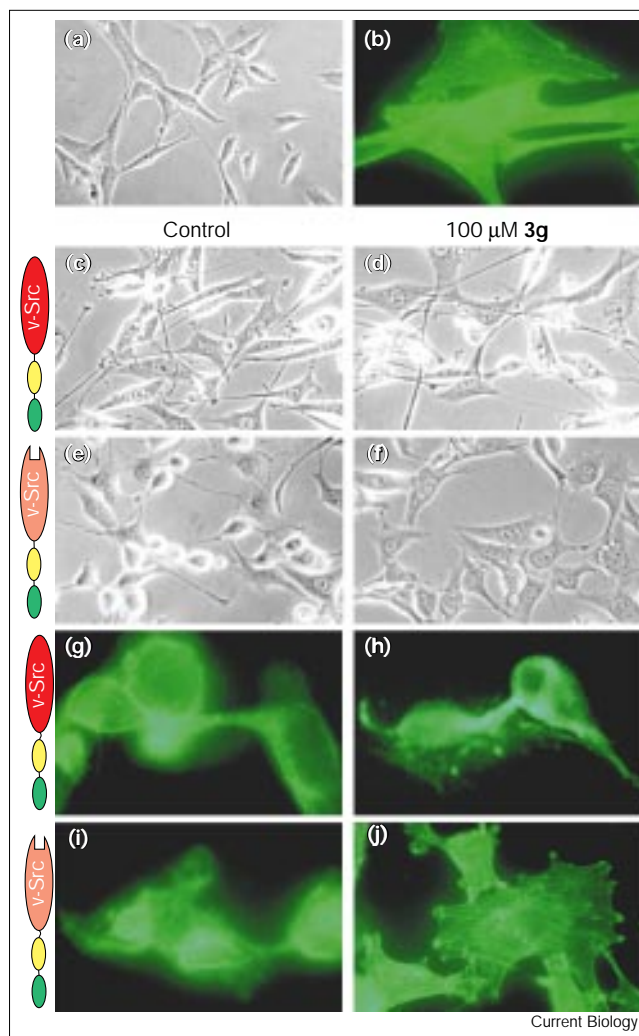
Generalization to other kinases

The advantage of using mutagenesis to provide a unique molecular difference between the enzyme of interest and all other enzymes is that the approach should be extendible across the kinase superfamily, because the kinase fold is conserved. Almost all known protein kinases contain a bulky side chain at the position corresponding to residue 338 of v-Src. A space-creating mutation at this position should therefore render any kinase susceptible to selective inhibition. To test this, we measured the inhibition of T339G Fyn by the analogues (Table 1). The structure–activity relationships of the analogues for I338G v-Src and T339G Fyn were found to be strikingly similar. The **3g** compound was the most potent inhibitor analogue against T339G Fyn, as it was for I338G v-Src, exhibiting an IC_{50} of 830 nM. This corresponds to greater than 300-fold selectivity for T339G Fyn over wild-type Fyn. The implication from these data is that multiple tyrosine kinases can be systematically engineered to accept one inhibitor analogue preferentially without the need to screen large libraries of putative inhibitors.

Conclusions

In this report, we describe a novel approach to selective protein kinase inhibition through the complementary engineering of kinases sensitive to specific chemicals and rationally designed inhibitors. We demonstrate that high selectivity for the target kinase can be achieved in whole cells, and that active-site inhibition of an oncogenic tyrosine kinase can be sufficient for the disruption of a transformed cell morphology. Because the approach is easily generalized, it should have far-reaching applications in deconvoluting signal-transduction pathways, as well as in the validation of kinases as targets for drug design. The pace of effective drug discovery is limited by the identification and

Figure 6



Fibroblasts transformed with I338G v-Src acquire a flattened morphology and regain actin stress fibers when they are incubated with **3g**. (a,b) Non-transformed, (c,d,g,h) wild-type v-Src-transformed, and (e,f,i,j) I338G v-Src-transformed NIH3T3 fibroblasts were treated with either 1.1% DMSO (a–c,e,g,i) or 100 μ M **3g** in 1.1% DMSO (d,f,h,j). After 48 h, cells were photographed (a,c–f), stained with FITC–phalloidin, and visualized by fluorescence microscopy (b,g–j).

validation of important drug targets. This is not a trivial problem in a milieu of homologous proteins that may potentially number 2000. The use of chemical-sensitive mutants of protein kinases expands the ability to probe the cellular and physiological effects of pharmacological kinase inhibition. As transfected cell lines and even ‘knock-in’ mice expressing a mutant protein of interest can now be generated rapidly, our approach should greatly expedite the process of testing the effects of selective inhibition of a given kinase in a whole-cell or animal model. As more inhibitor-bound protein kinase crystal structures become available, our strategy will allow for the systematic investigation of the effects of time-dependent and

dose-dependent inhibition of any given kinase in the scope of an entire signal transduction cascade.

Materials and methods

Chemical synthesis

All starting materials and synthetic reagents were purchased from Aldrich unless otherwise noted. All compounds were characterized by ^1H NMR and high resolution mass spectrometry. 4-amino-1-*tert*-butyl-3-phenylpyrazolo [3,4-*d*] pyrimidine (**2**) was synthesized according to Hanefeld *et al.* [32].

General procedure for N-4 acylation of 2 (3a–3g): To a solution of **2** (~100 mg) dissolved in 2 ml pyridine was added 10 equivalents of the desired acyl chloride at 0°C. The reaction mixture was allowed to warm to room temperature and stirred for 12 h. The reaction was quenched by the addition of 25 ml water. The resulting mixture was extracted with Et_2O and the combined Et_2O extracts were washed with 1 N HCl and 5% NaHCO_3 . The Et_2O layer was dried over MgSO_4 and evaporated. The residue was purified by flash chromatography on 25 g silica gel by elution with 1:1 Et_2O : hexanes to yield pure **3a–3g**.

4-cyclobutylamido-1-*tert*-butyl-3-phenylpyrazolo[3,4-*d*]pyrimidine (3a): Yield 0.0116 g (16%), white powder; HRMS (EI) molecular ion calculated for $\text{C}_{20}\text{H}_{23}\text{N}_5\text{O}$ 349.19049, found 349.18762; ^1H NMR (300 MHz, CDCl_3 , ppm) δ 1.86 (9H, s), 1.89–2.27 (6H, m), 3.58 (1H, m), 7.26–7.67 (5H, m), 8.69 (1H, s).

4-cyclopentylamido-1-*tert*-butyl-3-phenylpyrazolo[3,4-*d*]pyrimidine (3b): Yield 0.0456 g (68%), white powder; HRMS (EI) molecular ion calculated for $\text{C}_{21}\text{H}_{25}\text{N}_5\text{O}$ 363.20615, found 363.20398; ^1H NMR (270 MHz, CDCl_3 , ppm) δ 1.41–1.91 (8H, m), 1.87 (9H, s), 2.97 (1H, m), 7.51–7.67 (5H, m), 8.70 (1H, s).

4-cyclohexylamido-1-*tert*-butyl-3-phenylpyrazolo[3,4-*d*]pyrimidine (3c): Yield 0.0575 g (84%), white powder; ^1H NMR (270 MHz, CDCl_3 , ppm) δ 1.21–1.93 (10H, m), 1.86 (9H, s), 2.43 (1H, m), 7.51–7.67 (5H, m), 8.70 (1H, s).

4-2'-furylamido-1-*tert*-butyl-3-phenylpyrazolo[3,4-*d*]pyrimidine (3d): Yield 0.0342 g (60%), white powder; HRMS (EI) molecular ion calculated for $\text{C}_{20}\text{H}_{19}\text{N}_5\text{O}_2$ 361.15407, found 361.15254; ^1H NMR (270 MHz, CDCl_3 , ppm) δ 1.87 (9H, s), 6.52 (1H, d), 7.23 (1H, d), 7.43–7.53 (5H, m), 7.95 (1H, s), 8.59 (1H, s).

4-benzamido-1-*tert*-butyl-3-phenylpyrazolo[3,4-*d*]pyrimidine (3e): Yield 0.1309 g (56%), white powder; HRMS (EI) molecular ion calculated for $\text{C}_{22}\text{H}_{21}\text{N}_5\text{O}$ 371.17933, found 371.17324; ^1H NMR (270 MHz, CDCl_3 , ppm) δ 1.41–1.91 (8H, m), 7.22–8.11 (10H, m), 8.48 (1H, s).

4-(*p*-methyl)benzamido-1-*tert*-butyl-3-phenylpyrazolo[3,4-*d*]pyrimidine (3f): Yield 0.0751 g (33%), white powder; HRMS (EI) molecular ion calculated for $\text{C}_{23}\text{H}_{23}\text{N}_5\text{O}$ 385.19499, found 385.18751; ^1H NMR (270 MHz, CDCl_3 , ppm) δ 1.88 (9H, s), 2.42 (3H, s), 7.19 (2H, d), 7.41–8.11 (7H, m), 8.49 (1H, s).

4-(*p*-*tert*-butyl)benzamido-1-*tert*-butyl-3-phenylpyrazolo[3,4-*d*]pyrimidine (3g): Yield 0.1050 g (42%), white powder; HRMS (EI) molecular ion calculated for $\text{C}_{26}\text{H}_{29}\text{N}_5\text{O}$ 427.23747, found 427.23474; ^1H NMR (270 MHz, CDCl_3 , ppm) δ 1.35 (9H, s), 1.88 (9H, s), 7.38–7.99 (9H, m), 8.50 (1H, s).

General procedure for the reduction of N-4 acyl compounds to N-4 methylene compounds (4b, 4d, 4e): A round bottom flask was charged with ~30 mg LiAlH_4 . The flask was equipped with a pressure equalizing dropping funnel and flushed with dry argon. The LiAlH_4 was suspended in 3 ml THF over an ice bath. Approximately 100 mg of the corresponding N-4 acyl **2** analogue was dissolved in 5 ml THF and

added dropwise to the suspension of LiAlH_4 . The reaction mixture was stirred for 30 min on the ice bath and subsequently heated to reflux for 30 min. The reaction was quenched by the sequential, dropwise additions of 1 ml EtOAc , 1 ml water, and 1 ml 6 N NaOH . After stirring for 5 min, the reaction mixture was filtered through a celite pad, diluted with water and extracted with Et_2O . The Et_2O extracts were combined, dried over MgSO_4 , and evaporated. The residue was purified by flash chromatography on 10 g of silica gel by elution with 4:1 hexanes : EtOAc .

4-cyclopentylmethylamino-1-*tert*-butyl-3-phenylpyrazolo[3,4-*d*]pyrimidine (4b): Yield 0.0649 g (75%), clear oil; HRMS (EI) molecular ion calculated for $\text{C}_{21}\text{H}_{27}\text{N}_5$ 349.22691, found 349.22420; ^1H NMR (270 MHz, CDCl_3 , ppm) δ 1.16–2.14 (9H, m), 1.84 (9H, s), 3.54 (2H, d), 5.51 (1H, s), 7.46–7.67 (5H, m), 8.43 (1H, s).

4-2'-furylmethylamino-1-*tert*-butyl-3-phenylpyrazolo[3,4-*d*]pyrimidine (4d): Yield 0.0620 g (66%), beige powder; HRMS (EI) molecular ion calculated for $\text{C}_{20}\text{H}_{21}\text{N}_5\text{O}$ 347.17483, found 347.17330; ^1H NMR (270 MHz, CDCl_3 , ppm) δ 1.83 (9H, s), 4.75 (2H, d), 5.64 (1H, s), 6.25 (2H, d), 7.34–7.63 (6H, m), 8.45 (1H, s).

4-benzylamino-1-*tert*-butyl-3-phenylpyrazolo[3,4-*d*]pyrimidine (4e): Yield 0.0520 g (54%), white powder; HRMS (EI) molecular ion calculated for $\text{C}_{22}\text{H}_{23}\text{N}_5$ 357.19559, found 357.19303; ^1H NMR (270 MHz, CDCl_3 , ppm) δ 1.82 (9H, s), 4.76 (2H, d), 5.63 (1H, s), 7.28–7.63 (10H, m), 8.44 (1H, s).

Protein expression and purification

Site-directed mutagenesis and cloning of the genes for the glutathione-S-transferase fusion proteins of wild-type v-Src SH1 domain, I338G v-Src SH1, wild-type Fyn, T339G Fyn, and wild-type Abl into the pGEX-KT plasmid was carried out as described [23]. These kinases were expressed in DH5 α *Escherichia coli* and purified on immobilized glutathione beads (Sigma). PKA was purchased (Pierce) and used without further purification. PKC δ was expressed as the 6-His construct using the Bac-to-Bac expression system (pFastBac B vector). PKC δ was purified using a QIAexpress Ni–NTA agarose column.

In vitro kinase inhibition assay

IC_{50} values for putative kinase inhibitors were determined by measuring the counts per minute (cpm) of ^{32}P transferred to an optimized peptide substrate for Src family kinases (YGEFKKK, in single-letter amino-acid code). Various concentrations of inhibitor were incubated with 50 mM Tris (pH 8.0), 10 mM MgCl_2 , 1.6 mM glutathione, 1 mg/ml BSA, 133 μM YGEFKKK, 3.3% DMSO, 0.05 μM kinase and 11 nM (2 μCi) [γ - ^{32}P]ATP (6000 Ci/mmol, NEN) in a total volume of 30 μl for 30 min. Reaction mixtures (25 μl) were spotted onto a phosphocellulose disk, immersed in 10% HOAc, and washed with 0.5% H_3PO_4 . The transfer of ^{32}P was measured by standard scintillation counting. The IC_{50} was defined to be the concentration of inhibitor at which the cpm was 50% of the control disk. When the IC_{50} fell between two measured concentrations it was calculated based on the assumption of an inversely proportional relationship between inhibitor concentration and cpm between the two data points. Because the solubility limit of the inhibitor analogues in aqueous solutions is ~300 μM , IC_{50} values of ≥ 250 μM are approximate as full titrations to the upper limit of inhibition could not be tested. IC_{50} values for non-Src family kinases were measured equivalently with the following exceptions. Kemptide (Pierce, 133 $\mu\text{g}/\text{ml}$) was used as the substrate for PKA. An optimized Abl substrate (EAIYAAP-FAKKK, 133 $\mu\text{g}/\text{ml}$) was used for Abl assays. PKC δ assays were performed in the presence of 17 ng/ml diacyl glycerol (Sigma) and 17 ng/ml phosphatidyl serine (Sigma) with 170 ng/ml histone (Sigma) as the kinase substrate.

Murine B-cell assay

Splenic lymphocytes were isolated from 6–20 week old Balb/c or C57/B6 mice. The cells were washed out of the spleen into RPMI media containing 1 $\mu\text{g}/\text{ml}$ DNase I and the red-blood cells were lysed

in 17 mM Tris-ammonium chloride, pH 7.2. Approximately 4×10^6 cells were incubated at 37°C for 30 min with 100 μ M of **3g** or 2 in 1.1% DMSO. B-cell stimulation was initiated by the addition of 2 μ g of goat anti-mouse IgM (Jackson Immuno Research, 115-005-075) and subsequent incubation for 5 min at 37°C. The cells were isolated by centrifugation (13,000 rpm, 2 min) and lysed (lysis buffer: 1% Triton X-100, 50 mM Tris pH 7.4, 2 mM EDTA, 150 mM NaCl, 100 μ M PMSF, 2 mM sodium orthovanadate, 10 μ g/ml leupeptin, 10 μ g/ml aprotinin). The cellular debris was then pelleted at 13,000 rpm for 15 min. Cellular proteins were separated by 10% polyacrylamide gel electrophoresis and transferred to a nitrocellulose membrane by western blotting. Phosphotyrosine-containing proteins were visualized by immunoblotting with anti-phosphotyrosine antibody (Upstate Biotechnology).

Retroviral infection of NIH3T3 fibroblasts

Genes encoding wild-type and I338G v-Src were transfected into a packaging cell line and NIH3T3 fibroblasts were retrovirally infected using the pBabe retroviral vector and a puromycin (2.5 μ g/ml) selectable marker as described [36] (K.S., Y.L., K.M.S., unpublished observations). Cells transformed with wild-type and I338G v-Src were cultured in DMEM/10% BCS containing 2.5 μ g/ml puromycin.

Inhibition of v-Src in NIH3T3 fibroblasts

Non-transformed NIH3T3 cells and NIH3T3 cells transformed with wild-type v-Src or I338G v-Src were incubated at 37°C with 1.1% DMSO or 100 μ M **3g** in 1.1% DMSO. After 12 h, the cells were washed with PBS and lysed (lysis buffer: 1% Triton X-100, 50 mM Tris pH 7.4, 2 mM EDTA, 150 mM NaCl, 100 μ M phenylmethylsulphonyl fluoride, 2 mM sodium orthovanadate, 10 μ g/ml leupeptin, 10 μ g/ml aprotinin). The lysate was clarified by centrifugation at 13,000 rpm for 15 min. Lysate protein concentrations were normalized and equal volumes of the lysate were resolved by electrophoresis and analyzed for phosphotyrosine content as described above.

Microscopy

NIH3T3 fibroblasts that were non-transformed or transformed with wild-type or I338G were grown in DMEM/10% BCS on slides treated for tissue culture. Cells expressing v-Src were treated with either 1.1% DMSO or 100 μ M **3g** in 1.1% DMSO. After 48 h cells were photographed at 400 \times magnification through a Nikon TMS light microscope. Immediately following light microscopy, the cells were fixed for 20 min in 3.7% formaldehyde/PBS and permeabilized for 60 sec in 0.2% Triton X-100/PBS. Permeabilized cells were incubated with 200 ng/ml FITC-phalloidin/PBS for 20 min. Slides were rinsed with PBS and polymerized actin was visualized by fluorescence microscopy at 600 \times magnification on a Zeiss fluorescence microscope.

Acknowledgements

This research was supported by an NSF-Early Career Development Award (MCB-9506929) and the NIH (1R011CA70331-01). K.M.S. is a Pew Scholar in the biomedical sciences. We thank M. Eck for c-Src coordinates and J. Kuriyan for Hck coordinates, B. Drucker for providing antibody 4G10, T. Scanlan, P. Schultz, members of the laboratory, and particularly D. Kahne and S. Walker for their extremely helpful comments on the manuscript.

References

- Shokat KM: Tyrosine kinases: modular signaling enzymes with tunable specificities. *Chem Biol* 1995, 2:509-514.
- Thomas SM, Soriano P, Imamoto A: Specific and redundant roles of Src and Fyn in organizing the cytoskeleton. *Nature* 1995, 376:267-271.
- Bolen JB, Rowley RB, Spana C, Tsygankov AY: The Src family of tyrosine protein kinases in hemopoietic signal transduction. *FASEB J* 1992, 6:3403-3409.
- Ilic D, Furuta Y, Kanazawa S, Takeda N, Sobue K, Nakatsuji N, *et al.*: Reduced cell motility and enhanced focal adhesion contact formation in cells from FAK-deficient mice. *Nature* 1995, 377:539-544.
- Hunter T: A thousand and one protein kinases. *Cell* 1987, 50:823-829.
- Norman TC, Gray NS, Koh JT, Schultz PG: A structure-based approach to kinase inhibitors. *J Am Chem Soc* 1996, 118:7430-7431.
- Colas P, Cohen B, Jessen T, Grishina I, McCoy J, Brent R: Genetic selection of peptide aptamers that recognize and inhibit cyclin-dependent kinase 2. *Nature* 1996, 380:548-550.
- Groundwater PW, Solomons KRH, Drewe JA, Munawar MA: Protein tyrosine kinase inhibitors. *Prog Med Chem* 1996, 33:233-329.
- Levitski A, Gazit A: Tyrosine kinase inhibition: an approach to drug development. *Science* 1995, 267:1782-1787.
- Levitski A: SRC as a target for anti-cancer drugs. *Anticancer Drug Des* 1996, 11:175-182.
- Fry DW, Kraker AJ, McMichael A, Ambrosio LA, Nelson JM, Leopold WR, *et al.*: A specific inhibitor of the epidermal growth factor receptor tyrosine kinase. *Science* 1994, 265:1093-1095.
- Traxler P, Bold G, Frei J, Lang M, Lydon N, Mett H, *et al.*: Use of a pharmacophore model for the design of EGF-R tyrosine kinase inhibitors: 4-(phenylamino)pyrazolo[3,4-d]pyrimidines. *J Med Chem* 1997, 40:3601-3616.
- Buchdunger E, Zimmermann J, Mett H, Meyer T, Muller M, Regenass U, *et al.*: Selective inhibition of the platelet-derived growth factor signal transduction pathway by a protein-tyrosine kinase inhibitor of the 2-phenylaminopyrimidine class. *Proc Natl Acad Sci USA* 1995, 92:2558-2562.
- Hamby JM, Connolly CJ, Schroeder MC, Winters RT, Showalter HD, Panek RL, *et al.*: Structure-activity relationships for a novel series of pyrido[2,3-d]pyrimidine tyrosine kinase inhibitors. *J Med Chem* 1997, 40:2296-2303.
- Mohammadi M, McMahon G, Sun L, Tang C, Hirth P, Yeh BK, *et al.*: Structures of the tyrosine kinase domain of fibroblast growth factor receptor in complex with inhibitors. *Science* 1997, 276:955-960.
- Traxler P, Furet P, Mett H, Buchdunger E, Meyer T, Lydon N: Design and synthesis of novel tyrosine kinase inhibitors using a pharmacophore model of the ATP-binding site of the EGF-R. *J Pharm Belg* 1997, 52:88-96.
- Druker BJ, Tamura S, Buchdunger E, Ohno S, Segal GM, Fanning S, *et al.*: Effects of a selective inhibitor of the abl tyrosine kinase on the growth of bcr-abl positive cells. *Nat Med* 1996, 2:561-566.
- Brown MT, Cooper JA: Regulation, substrates and functions of src. *Biochim Biophys Acta* 1996, 1287:121-149.
- Hanke JH, Gardner JP, Dow RL, Changelian PS, Brissette WH, Weringer EJ, *et al.*: Discovery of a novel, potent, and src family-selective tyrosine kinase inhibitor. *J Biol Chem* 1996, 271:695-701.
- Li Z, Burke TR, Bolen JB: Analysis of styryl-based inhibitors of the lymphocyte tyrosine protein kinase p56^{lck}. *Biochem Biophys Res Commun* 1991, 180:1048-1056.
- Stein PL, Lee HM, Rich S, Soriano P: pp59^{lyn} mutant mice display differential signaling in thymocytes and peripheral T cells. *Cell* 1992, 70:741-750.
- Hanks SK, Quinn AM: Protein kinase catalytic domain sequence database: identification of conserved features of primary structure and classification of family members. *Methods Enzymol* 1991, 200:38-62.
- Shah K, Liu Y, Deirmengian C, Shokat KM: Engineering unnatural nucleotide specificity for Rous sarcoma virus tyrosine kinase to uniquely label its direct substrates. *Proc Natl Acad Sci USA* 1997, 94:3565-3570.
- Liu Y, Shah K, Yang F, Witucki L, Shokat K: Engineering src family protein kinases with unnatural nucleotide specificity. *Chem Biol* 1998, 5:91-101.
- Sicheri F, Moarefi I, Kuriyan J: Crystal structure of the src family tyrosine kinase hck. *Nature* 1997, 385:602-609.
- Xu W, Harrison SC, Eck MJ: Three-dimensional structure of the tyrosine kinase c-Src. *Nature* 1997, 385:595-601.
- Knighton DR, Zheng JH, Ten-Eyck LF, Ashford VA, Zuong NH, Taylor SS, *et al.*: Crystal structure of the catalytic subunit of cyclic adenosine monophosphate regulated protein kinase. *Science* 1991, 253:407-414.
- Zheng J, Knighton DR, Ten Eyck LF, Karlsson R, Zuong N-H, Taylor SS, *et al.*: Crystal structure of the catalytic subunit of cAMP-dependent protein kinase complexed with MgATP and peptide inhibitor. *Biochemistry* 1993, 32:2154-2161.
- Hardie G, Hanks S: *The Protein Kinase Facts Book: Protein-tyrosine Kinases*. San Diego: Academic Press Inc; 1995.

30. Jacobson KA, van Galen PJM, Williams M: Adenosine receptors: pharmacology, structure-activity relationships, and therapeutic potential. *J Med Chem* 1992, 35:407-422.
31. Graziani Y, Erikson E, Erikson RL: The effect of quercetin on the phosphorylation activity of the rous sarcoma virus transforming gene product *in vitro* and *in vivo*. *Eur J Biochem* 1983, 135:583-589.
32. Hanefeld U, Rees CW, White AJP, Williams DJ: One-pot synthesis of tetrasubstituted pyrazoles - proof of regiochemistry. *J Chem Soc Perkin Trans 1* 1996, 1996:1545-1552.
33. Kobayashi S: The synthesis and xanthine oxidase inhibitory activity of pyrazolo[3,4-d]pyrimidines. *Chem Pharm Bull (Tokyo)* 1973, 21:941-951.
34. Cambier JC, Jensen WA: The hetero-oligomeric antigen receptor complex and its coupling to cytoplasmic effectors. *Curr Opin Genet Dev* 1994, 4:55-63.
35. Bishop AC, Moore D, Scanlan TS, Shokat KM: Screening a hydroxystilbene library for selective inhibition of the B cell antigen receptor kinase cascade. *Tetrahedron* 1997, 53:11995-12004.
36. Morgenstern JP, Land H: Advanced mammalian gene transfer: high titre retroviral vectors with multiple drug selection marker and a complementary helper-free packaging line. *Nucleic Acids Res* 1990, 18:3587-3596.
37. Bellagamba C, Hubaishy I, Bjorge JD, Fitzpatrick SL, Fujita DJ, Waisman DM: Tyrosine phosphorylation of annexin II tetramer is stimulated by membrane binding. *J Biol Chem* 1997, 272:3195-3199.
38. Martin GS: Rous sarcoma virus: a function required for the transformed state. *Nature* 1970, 227:1021-1023.
39. Jakobovits EB, Majors JE, Varmus HE: Hormonal regulation of the rous sarcoma virus *src* gene via a heterologous promoter defines a threshold dose for cellular transformation. *Cell* 1984, 38:757-765.
40. Kwon HJ, Yoshida M, Fukui Y, Horinouchi S, Beppu T: Potent and specific inhibition of p60 v-src protein kinase both *in vivo* and *in vitro* by radicicol. *Cancer Res* 1992, 52:6926-6930.
41. Whitesell L, Shifrin SD, Schwab G, Neckers LM: Benzoquinoid ansamycins possess selective tumoricidal activity unrelated to *src* kinase inhibition. *Cancer Res* 1992, 52:1721-1728.
42. Stebbins CE, Russo AA, Schneider C, Rosen N, Hartl FU, Pavletich NP: Crystal structure of an hsp90-geldanamycin complex: targeting of a protein chaperone by an antitumor agent. *Cell* 1997, 89:239-250.
43. Whitesell L, Mimnaugh EG, De Costa B, Myers CE, Neckers LM: Inhibition of heat shock protein hsp90-pp60^{v-src} heteroprotein complex formation by benzoquinone ansamycins: essential role for stress proteins in oncogenic transformation. *Proc Natl Acad Sci USA* 1994, 91:8324-8328.
44. Sepp-Lorenzino L, Ma Z, Lebwohl DE, Vinitzky A, Rosen N: Herbimycin A induces the 20 S proteasome- and ubiquitin-dependent degradation of receptor tyrosine kinases. *J Biol Chem* 1995, 270:16580-16587.

Because **Current Biology** operates a 'Continuous Publication System' for Research Papers, this paper has been published on the internet before being printed. The paper can be accessed from <http://biomednet.com/cbiology/cub> – for further information, see the explanation on the contents page.